High-Q Microresonator as a Five-Partite Entanglement Generator via Cascaded Parametric Processes

Yutian Wen[1], Qiang Lin[2], Guangqiang He[1†]

[1]*State Key Lab of Advanced Optical Communication Systems and Networks, Department of Electronic Engineering, Shanghai Jiao Tong University, Shanghai 200240, China*

[2]*Department of Elctrical and Computer Engineering, University of Rochester, NY 14627, USA*

Introduction

- Quantum computation is expected to provide exponential speedup for particular mathematical problems such as integer factoring and quantum symtem simulation.
- The generation of a scalable cluster state, which is a special multipartite entanglement[1], is the main challenge of the one-way quantum computation model.
- Optical frequency comb (OFC) is proved to be capable of carrying cluster states, which can be used to implement quantum information processing[2], quantum teleportation network[3], quantum cryptographic network[4].
- The conventional way to generate an OFC is to use the mode-locked lasers that are usually bulky, difficult to operate, and susceptible to environmental perturbations.
- It is recently reported that OFCs can also be generated from high-Q monolithic microresonators through cascaded four-wave mixing (FWM).
- Advantages: 1. compatibility with CMOS technologies; 2. longer life time thus more significant quantum effect.
- The multipartite quantum entanglement relationship between different comb modes generated from high-Q microresonators are yet to be discovered.
- The purpose of our work [5] is to analyze the five-partite entanglement between OFCs generated from high-Q microresonators.

System model

- Optical frequency comb: An OFC is a light source composed of equally spaced discrete frequency components. Actual OFCs might extend to an extremely broad band with hundreds of frequency components, each of which corresponds to a comb mode.

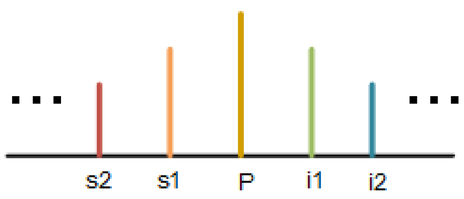

- Experimental scheme: We consider a generic scheme of comb generation, where a continuous-wave pump wave is launched into a microresonator to excite FWM process. The resulting frequency comb output from the cavity is then separated into individual frequency components for analysis.

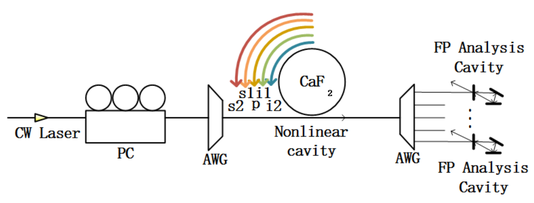

- To generate OFCs via cascaded FWM processes: In a high-Q microresonator, an intense pump wave launched into a cavity mode would excite four-wave mixing processes among different cavity modes via the optical Kerr effect. The iteration of degenerate and non-degenerate FWM processes thus produce an optical frequency comb, with a spectral extent determined by the group-velocity dispersion of the device.

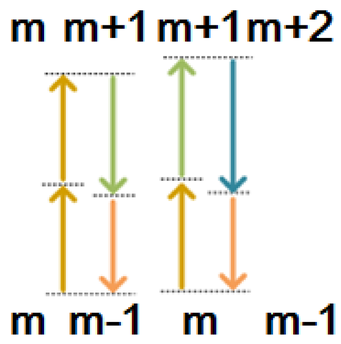

- The FWM process governing the comb generation originates from the optical Kerr effect. With an electric field composed of five frequency components, the interaction Hamiltonian of the Kerr effect is given by

$$V = \hbar(g/2) : (a_p + a_{s1} + a_{i1} + a_{s2} + a_{i2} + \text{H.c.})^4 :, \quad (1)$$

where ": ... :" stands for normal ordering and g is coupling coefficient given as

$$g = \frac{n_2 \hbar \omega_0^2 c}{\mathcal{V} n_0^2}, \quad (2)$$

where n_2 is nonlinear refractive index that characterizes the strength of the optical nonlinearity, n_0 is the linear refractive index of the material, c is the speed of light in the vacuum, and $\mathcal{V}$ is the effective mode volume.

- Hamiltonian for the comb generation system is found to be

$$H = H_{\text{free}} + H_{\text{pump}} + H_{\text{int}}, \quad (3)$$

$$H_{\text{free}} = \hbar \sum_k \omega_k a_k^\dagger a_k, \; H_{\text{pump}} = i\hbar\epsilon a_p^\dagger + \text{H.c.}, \quad (4)$$

$$H_{\text{int}} = i\frac{g}{2}\hbar \sum_k a_k^\dagger a_k^\dagger a_k a_k + ig\hbar \sum_{k\neq t} a_k^\dagger a_t^\dagger a_t a_k + ig\hbar(a_{s1}^\dagger a_{i1}^\dagger a_p^2 + a_{s2}^\dagger a_{i1}^\dagger a_{s1} a_p + a_{s1}^\dagger a_{i2}^\dagger a_{i1} a_p + a_{s2}^\dagger a_p^\dagger a_{s1}^2 + a_{i2}^\dagger a_p^\dagger a_{i1}^2) + \text{H.c.}, \quad (5)$$

where $k, t = p, s1, s2, i1, i2$ and ϵ is the pump field that enters the resonator which is described classically because of its intense amplitude.

- Processes $2\omega_p \rightarrow \omega_{s2} + \omega_{i2}$ and $\omega_{s1} + \omega_{i1} \rightarrow \omega_{s2} + \omega_{i2}$ are neglected from our interaction Hamiltonian because they play relatively minor roles compared to other terms due to larger phase mismatch and the smaller intensities of $s1$ and $i1$ compared to the pump.
- Damping term

$$L_k\rho = \gamma_k(2a_k\rho a_k^\dagger - a_k^\dagger a_k \rho - \rho a_k^\dagger a_k), \quad (6)$$

in which ρ is the density matrix of the five modes under consideration. $\gamma_k = \gamma_{k0} + \gamma_{kc}$ stands for the damping rate of the loaded cavity. We assume that the five comb modes exhibit the same photon decay rate and the same external coupling rate ($\gamma_k = \gamma, \gamma_{kc} = \gamma_c, \gamma_{k0} = \gamma_0, k = p, s1, s2, i1, i2$), since their frequencies are not far from each other.

- Input-output relations The output fields are determined by the well-known input-output relations given as

$$b_{out} - b_{in} = \sqrt{\gamma} a, \quad (7)$$

where b is the boson annihilation operator for the bath field outside the cavity.

Equations of Motion for the Full Hamiltonian

The master equation for the five cavity modes (with rotating-wave approximation $a_k \rightarrow \mathrm{e}^{-\mathrm{i}\omega_k t} a_k$)

$$\frac{\partial \rho}{\partial t} = -\frac{i}{\hbar}[H_{\text{pump}} + H_{\text{int}}, \rho] + \sum_{k=1}^{5} L_k \rho. \quad (8)$$

The master equation above can be converted into the equivalent c-number Fockker-Planck equation in P representation, which can be written as a completely equivalent stochastic differential equation as

$$\frac{\partial \alpha}{\partial t} = \mathbf{F} + \mathbf{B}\eta, \quad (9)$$

where $\alpha = [\alpha_{\mathbf{p}}, \alpha_{\mathbf{s1}}, \alpha_{\mathbf{i1}}, \alpha_{\mathbf{s2}}, \alpha_{\mathbf{i2}}, \alpha_{\mathbf{p}}^*, \alpha_{\mathbf{s1}}^*, \alpha_{\mathbf{i1}}^*, \alpha_{\mathbf{s2}}^*, \alpha_{\mathbf{i2}}^*]^{\mathbf{T}}$, and $\mathbf{F} = [\mathbf{f}, \mathbf{f}^*]^{\mathbf{T}}$ is the main part of the system's evolution.

Matrix $\mathbf{B}$ contains the coefficients of the noise terms which is obtained through $\mathbf{B}\mathbf{B}^{\mathbf{T}} = \mathbf{D}$ in which the diffusion matrix $\mathbf{D}$ is given in ref. [5] In Eq. (9), $\eta = [\eta_1(\mathbf{t}), \eta_2(\mathbf{t}), \eta_3(\mathbf{t}), \eta_4(\mathbf{t}), \eta_5(\mathbf{t}), \mathbf{c.c.}]^{\mathbf{T}}$, where η_i are real noise terms characterized by $\langle \eta_i(t) \rangle = 0$ and $\langle \eta_i(t)\eta_j(t) \rangle = \delta_{ij}\delta(t - t')$.

Linearized Quantum-Fluctuation Analysis

Decompose the system variables into their steady-state (classical) values and quantum fluctuations as $\alpha_i = A_i + \delta\alpha_i$.

Steady-state solution The steady state of the comb generation can be found by setting $\partial\alpha/\partial\mathbf{t}$ in Eq. (9) to be zero.

$$\epsilon_{th} = \gamma\sqrt{\gamma/g}, \quad (10)$$

$$A_p = \frac{\varepsilon + \sqrt{\varepsilon^2 + (3\gamma^3)/g}}{3\gamma}, \quad (11)$$

$$A_{i1} = A_{s1} = A_a = \sqrt{\frac{\gamma}{4g}(1 - \frac{\gamma}{gA_p^2})}, \quad (12)$$

$$A_{i2} = A_{s2} = A_b = \frac{2gA_pA_a^2}{\gamma}. \quad (13)$$

ϵ_{th} is the threshold of pump. Only when the pump power is above this threshold will the rest of the comb components appears.

Quantum fluctuation correlation With the steady-state solution, we can find the equations of motion governing the quantum fluctuations of the comb modes as

$$\frac{\partial}{\partial t}\delta\alpha = \mathbf{M}\delta\alpha + \mathbf{B}\eta, \quad (14)$$

where $\delta\alpha = [\delta\alpha_{\mathbf{p}}, \delta\alpha_{\mathbf{s1}}, \delta\alpha_{\mathbf{i1}}, \delta\alpha_{\mathbf{s2}}, \delta\alpha_{\mathbf{i2}}, \text{H.c.}]^{\mathbf{T}}$. M is the drift matrix which is defined in Ref.[5].

The fluctuation equations describe an Ornstein-Uhlenbeck process for which the intracavity spectral correlation matrix is

$$\mathbf{S}(\omega) = (-\mathbf{M} + \mathrm{i}\omega\mathbf{I})^{-1}\mathbf{D}(-\mathbf{M}^{\mathbf{T}} - \mathrm{i}\omega\mathbf{I})^{-1}. \quad (15)$$

All the correlations required to study the measurable extracavity spectra are then contained in this intracavity spectral matrix.

In order to investigate the multipartite entanglement, we define quadrature operators for each mode as

$$X_k = a_k + a_k^\dagger, \; Y_k = -i(a_k - a_k^\dagger), \quad (16)$$

with a commutation relationship of $[X_k, Y_k] = 2i$. Based on such definition, $V(X_k) \leq 1$ will indicate a squeezed state, where $V(A) = \langle A^2 \rangle - \langle A \rangle^2$ denotes the variance of operator A. Accordingly, by use of Eq. (7), the spectral variances and covariances of the output fields have the general form

$$\begin{cases} S_{X_i}^{out}(\omega) = 1 + 2\gamma_c S_{X_i}(\omega) \\ S_{X_i,X_j}^{out}(\omega) = 2\gamma_c S_{X_i,X_j}(\omega). \end{cases} \quad (17)$$

Similar expressions can be derived for the Y quadratures.

Five-partite Entanglement Criteria

The condition proposed by van Loock and Furusawa (VLF), which is a generalization of the conditions for bipartite entanglement, is sufficient to demonstrate multipartite entanglement. We now demonstrate how these may be optimized for the verification of genuine five-partite entanglement in this system. Using the quadrature definitions, the five-partite inequalities, which must be simultaneously violated, are

$$S_{(1)} = V(X_p + X_{s1}) + V(-Y_p + Y_{s1} + g_{i1}Y_{i1} + g_{s2}Y_{s2} + g_{i2}Y_{i2}) \geq 4, \quad (18)$$

$$S_{(2)} = V(X_p + X_{i1}) + V(-Y_p + g_{s1}Y_{s1} + Y_{i1} + g_{s2}Y_{s2} + g_{i2}Y_{i2}) \geq 4, \quad (19)$$

$$S_{(3)} = V(X_{s1} - X_{s2}) + V(g_pY_p + Y_{s1} + g_{i1}Y_{i1} + Y_{s2} + g_{i2}Y_{i2}) \geq 4, \quad (20)$$

$$S_{(4)} = V(X_{i2} - X_{i1}) + V(g_pY_p + g_{s1}Y_{s1} + Y_{i1} + g_{s2}Y_{s2} + Y_{i2}) \geq 4, \quad (21)$$

where the g_k ($k = p, s1, s2, i1, i2$) are arbitrary real parameters that are used to optimize the violation of these inequalities. Due to the symmetry relation between signal and idler photons, Eq. (18) and Eq. (19) are equivalent. So are Eq. (20) and Eq. (21).

Numerical simulation and discussion

Through careful calculation, we find that the extracavity entanglement is completely determined by three independent parameters: $\varepsilon/\varepsilon_{th}$, γ_c/γ and ω/γ.

From now on, we numerically calculate the values of VLF inequalities. The list of assumptions:

- Spherical $\mathrm{CaF_2}$ cavity. Refractive index $n_0 = 1.43$, Kerr coefficient $n_2 = 3.2 \times 10^{-20}\ \mathrm{m^2/W}$.
- The radius R of the microresonator is $2.5\ \mathrm{mm}$, corresponding to an effective mode volume of $V_0 = 6.6 \times 10^{-12}\ \mathrm{m^3}$.
- Light is critically coupled to the device with a loaded quality factor $Q_0 = 3 \times 10^9$, corresponding to a central modal bandwidth $\Delta\omega_0 = \gamma_p \approx 2\pi \times 64\ \mathrm{kHz}$)
- Pump wavelength $\lambda_0 = 1560.5\ \mathrm{nm}$.

Effect of the External Coupling Rate

Fix g, γ and ϵ and vary the γ_c/γ ratio. We plot the minimum of the variances versus the analysis frequency normalized to γ when γ_c takes a portion of $0.34, 0.57, 0.8, 1$ of the total damping rate. The blue dashed lines stand for $S_{(1)}$, while the green solid ones stand for $S_{(3)}$.

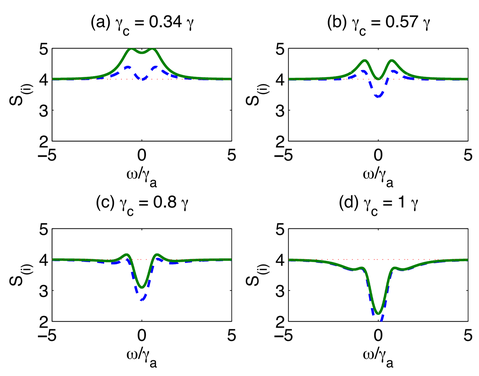

- The entanglement among output modes are improved as the γ_c/γ ratio increase, i.e., the entanglement is better when the cavity has higher Q therefore lower intracavity loss, and higher extracavity coupling coefficient.
- This can be interpreted naturally if we see the coupling as a beam splitter which extract squeezed quantum noise to the output, so the higher portion the coupling coefficient takes in the total damping rate, the less consumed entangled pair of photons are wasted in the internal loss.

Effect of the Pump Power We plot the minimal variance throughout the noise power spectrum as a function of the pump power (normalized by ϵ_{th})) and six typical spectrums.

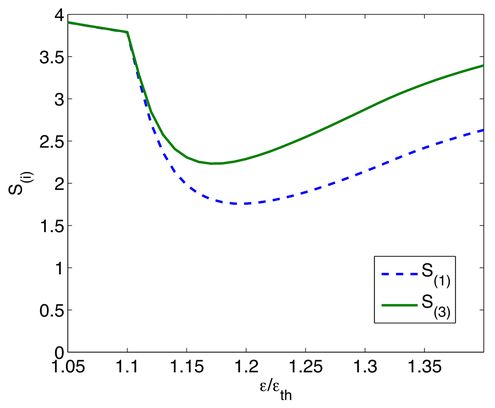

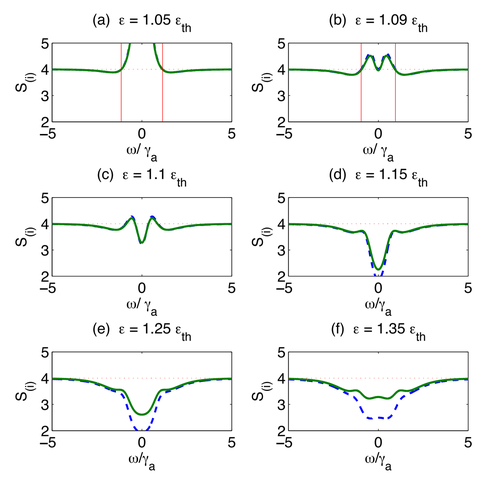

- Both variance first descend as the pump power increases, then ascend. $S_{(3)}$ and $S_{(4)}$ reaches their global minimum at $\epsilon = 1.15\epsilon_{\text{th}}$, therefore $1.15\epsilon_{\text{th}}$ is the optimal pump power.
- The other turning point is around $1.1\epsilon_{\text{th}}$, when, as we can see in Fig. (b) and (c), the variances in the center frequency begin to decrease dramatically and become the minimum which was once achieved in the side band, as showed in Fig. (a).

References

[1] Y. Gu, G. Q. He, X. F. Wu, Phys. Rev. A **85,** 052328(2012).

[2] J. T. Zhang, G. Q. He, and G. H. Zeng, Phys. Rev. A **80,** 052333(2009).

[3] L. J. Ren, G. Q. He, and G. H. Zeng, Phys. Rev. A **78,** 042302(2008).

[4] Y. J. Qian, Z. Shen, G. Q. He and G. H. Zeng, Phys. Rev. A **86,** 052333(2012).

[5] Y. T. Wen, X. F. Wu, R. Y. Li, Q. Lin and G. Q. He, Phys. Rev. A **91**, 042311(2015).

† Contact information: Guangqiang He, Room 1-313 SEIEE Buildings, Department of Electronic Engineering, Shanghai JiaoTong University, Shanghai, PRC 200240 – Phone: 86-21-34208104 – Email: *guangqianghe@gmail.com*; Web: *www.sjtu.edu.cn*

Acknowledgments: This work is supported by the National Natural Science Foundation of China (Grant Nos. 61475099, 61102053), Program of State Key Laboratory of Quantum Optics and Quantum Optics Devices (No. KF201405), the Scientific Research Foundation for the Returned Overseas Scholars, State Education Ministry, SMC Excellent Young Faculty program, SJTU.